A numerical study on the circulation, wave and suspended sediment in the Yellow and East China Seas

Kyeong Ok Kim[1], Igor Brovchenko[2], Vladimir Maderich[2], Hanna Kim[1], Mee Kyung Kim[1], Kyung Tae Jung[1]
[1]Korea Institute of Ocean Science & Technology, Busan, Korea (kokim@kiost.ac.kr)
[2]Institute of Mathematical Machine and Systems Problems, Kiev, Ukraine

ABSTRACT

We summarize in this work a recent development of a SELFE-based three-dimensional numerical model for the Yellow and East China Seas (YSECS) equipped with multiple-scale circulation, wave and multiple-size suspended sediment modules. Some important improvements have been made. To deal with the multiple-scale circulation, we have introduced an open boundary condition to obtain stable solutions in the presence of multi-scale circulation. We have extended the non-cohesive sediment module of SELFE to the form applicable to mixture of cohesive and non-cohesive sedimentary regimes by implementing an extended form of erosional rate and a flocculation model for the determination of settling velocity of cohesive flocs. We assume that erosion of mixtures of cohesive (mud) and non-cohesive sediments (sand) is independent if clay content is below critical. Above critical clay content the bed behaves cohesively. In the non-cohesive regime exchange of sand and mud with bottom is independent, whereas in cohesive regime an erosion of mud and sand occurs simultaneously as cohesive sediment. The deposition is independent process for cohesive and non-cohesive sediments. Results of suspended sediment distributions in the Yellow Sea computed without wave and with wave have been compared with newly constructed GOCI images.

INTRODUCTION

High turbidity plays an important role in controlling the pollutant distribution and ecosystem dynamics in the YSECS. Nevertheless, observational and modeling studies on the suspended sediment distribution in the YSECS were very limitedly performed. To the authors' knowledge, Choi et al (2005a, b) carried out unique numerical studies by taking into account mixture of cohesive and non-cohesive sediments. In detail, they investigated the sedimentary dynamics in the Yellow and East China Seas using a 3D finite-difference model with 5 minute resolution on the horizontal plane and 5 sigma layers in the vertical direction, considering transport processes of cohesive and non-cohesive sediment (fine sand) as well as the hydrodynamic processes associated with tides, meteorological forcing and waves. Thermohaline effects were however excluded although suspended sediment discharges through rivers were included. Model results were compared with shipboard observations off Changjiang estuary.

In this works we numerically investigate the transport of suspended sediment in YSECS by additionally taking into account the oceanic circulation and making comparison with GOCI satellite data. Cohesive and non-cohesive sediments are considered together. The finite element model with minimum horizontal mesh size of about 400m and 20 vertical layers composed of 11 *s*-coordinate layers and 9 *z*-coordinate layers) has been used and attention has been paid to the comparison of model results computed with and without waves.

MODEL DESCRIPTION

3D Baroclinic Circulation Model

For the calculation of 3D baroclinic circulation the model SELFE has been used. Here details of the model are omitted; only the open boundary condition is described. Along the open boundary, a mixed form of open boundary condition (clamped elevation boundary condition plus relaxation boundary condition for the velocity) is newly added.

$$\eta_b = \eta_h + \eta_t$$

$$\vec{v}_b = \alpha(\vec{v}_h + \vec{v}_t) + (1-\alpha)\vec{v}_m$$

Here $\eta_h(\vec{x},t)$ is the free surface elevation from the global model, η_t is the tidal free surface elevation on the boundary, $\vec{v}_h(\vec{x},t)$ is the 3D globally calculated velocity field, $\vec{v}_t$ is the tidal barotropic velocity field, $\vec{v}_m$ is the model simulated value of the boundary velocity, α is the relaxation parameter.

3D Sediment Transport Model

Sediment transport in the water column is described by advection-diffusion equation:

$$\frac{\partial C_j}{\partial t} + \frac{\partial}{\partial x_i}(u_i C_j) = \frac{\partial}{\partial x_i}(k_i \frac{\partial C_j}{\partial x_i}) + w_{sj}\frac{\partial C_j}{\partial z}, \quad i = 1,2;$$

where C_j is the volume concentration of suspended sediment in class *j*; x_1 and x_2 are the horizontal coordinates, z is the vertical coordinate; u_i is the velocity components on the horizontal plane, k_i is the eddy diffusivity coefficients; w_{sj} is the settling velocity of suspended sediment in class *j*.

Bottom boundary conditions representing the exchange of sediment between the bed and flow are defined by

$$k_3 \frac{\partial C_j}{\partial z} + w_{sj} C_j = -D_j + E_j \quad \text{at } z = -H;$$

where D_j is the deposition flux of sediments of class *j*; E_j is the erosion flux of sediments of class *j*; H is the water depth.

Deposition and Erosion of Non-cohesive Sediment

Deposition of non-cohesive sediment $(j \geq 1)$ is given by

$$D_j = w_{sj} C_j(-H);$$

where $C_j(-H)$ is the concentration in bottom computational cell of sediments of class *j*.

Erosion flux is calculated using van Rijn(1984) formulation.

$$E_j = E_{0,j}(d_i)(1-p) f_j \{\tau_b/\tau_{cr,j} \cdot (1+f_0)^{-1} - 1\}^{1.5} \text{ when } \tau_b > \tau_{cr,j};$$

where $E_{0,j}(d_i) = (\rho_s/a)\cdot(0.015 d_i / D_*^{0.3})$ is the erosion rate; d_i is the sediment particle diameter, $D_* = g(\rho_s/\rho_w - 1)^{1/3}\nu^{-2/3}$; p is porosity; f_j and f_0 are volume fractions of sediment class *j* and cohesive sediments in the bed; τ_b is bottom shear stress; $\tau_{cr,j}$ is critical shear stress for sediment class *j*; $a = 3d_i$ is reference level above bottom.

Deposition and Erosion of Cohesive Sediment

Deposition flux of the cohesive sediment $(j = 0)$ appears only if shear stress is less than critical shear stress for deposition:

$$D_j = w_{sj} C_j(-H)(1 - \tau_b/\tau_{crd,j}) \text{ when } \tau_b < \tau_{crd,j},$$

where $\tau_{crd,j}$ is critical shear stress for the deposition of cohesive sediment.

Erosion flux of the cohesive sediment is formulated following Ariathurai and Arulanandan (1978).

$$E_j = E_{0,j}(1-p) f_j (\tau_b/\tau_{cre,j} - 1) \text{ when } \tau_b/\tau_{cre,j},$$

where $\tau_{cre,j}$ is critical shear stress for the erosion of cohesive sediment.

For the mixture of cohesive and non-cohesive sediments we follow the approach by van Ledden (2002). It is based on the critical cohesive sediment fraction in the bed $f_{cr,j}\,(j=0)$. If cohesive sediment fraction in the bed is above critical $(f_j > f_{cr,j})$, erosion and deposition occur in cohesive regime, while below critical $(f_j < f_{cr,j})$, erosion and deposition occur in non-cohesive regime.

Considering floc formation, settling velocity of cohesive sediment is determined as:

$$w_{sj} = (\rho_s - \rho_w)\cdot(D_p/D_f)\cdot g/(\rho_w \cdot 18\nu)\cdot D_f^2/(1 + 0.15\,\mathrm{Re}^{0.687}),$$

$$\mathrm{Re} = w_{sj} D_f / \nu,$$

where ρ_s is the primary particle density, ρ_w is water density, D_p is diameter of primary particles, D_f is the floc diameter, g is gravity, and ν is water viscosity,

Wave Model

The 3rd generation spectral wave model (WWM-II) embedded in SELFE system is used (Roland et al, 2012).

The wave action equation in the system reads:

$$\frac{\partial N}{\partial t} + \frac{\partial}{\partial x}(c_x N) + \frac{\partial}{\partial y}(c_y N) + \frac{\partial}{\partial \sigma}(c_\theta N) + \frac{\partial}{\partial \theta}(c_\sigma N) = S_{tot}$$

where $N = N(t,x,y,\sigma,\theta)$ is the wave action density spectrum; t is time; c_x and c_y are the wave propagation velocities in x and y directions, respectively; c_σ and c_θ are the wave propagation velocities in σ and θ directions, respectively; σ is the relative wave frequency, θ is the wave direction; S_{tot} is the source functions.

Application To the Yellow and East China Sea

Model Setup

The model domain covers most of shelf sea regions of YSECS with open boundaries near the Taiwan Strait, Ryukyu Islands and Korea Strait. Hydrodynamic model mesh was constructed using 50,613 nodes and 96,217 triangle elements (Fig. 1). The best resolution 400m is along Korea and China shorelines.

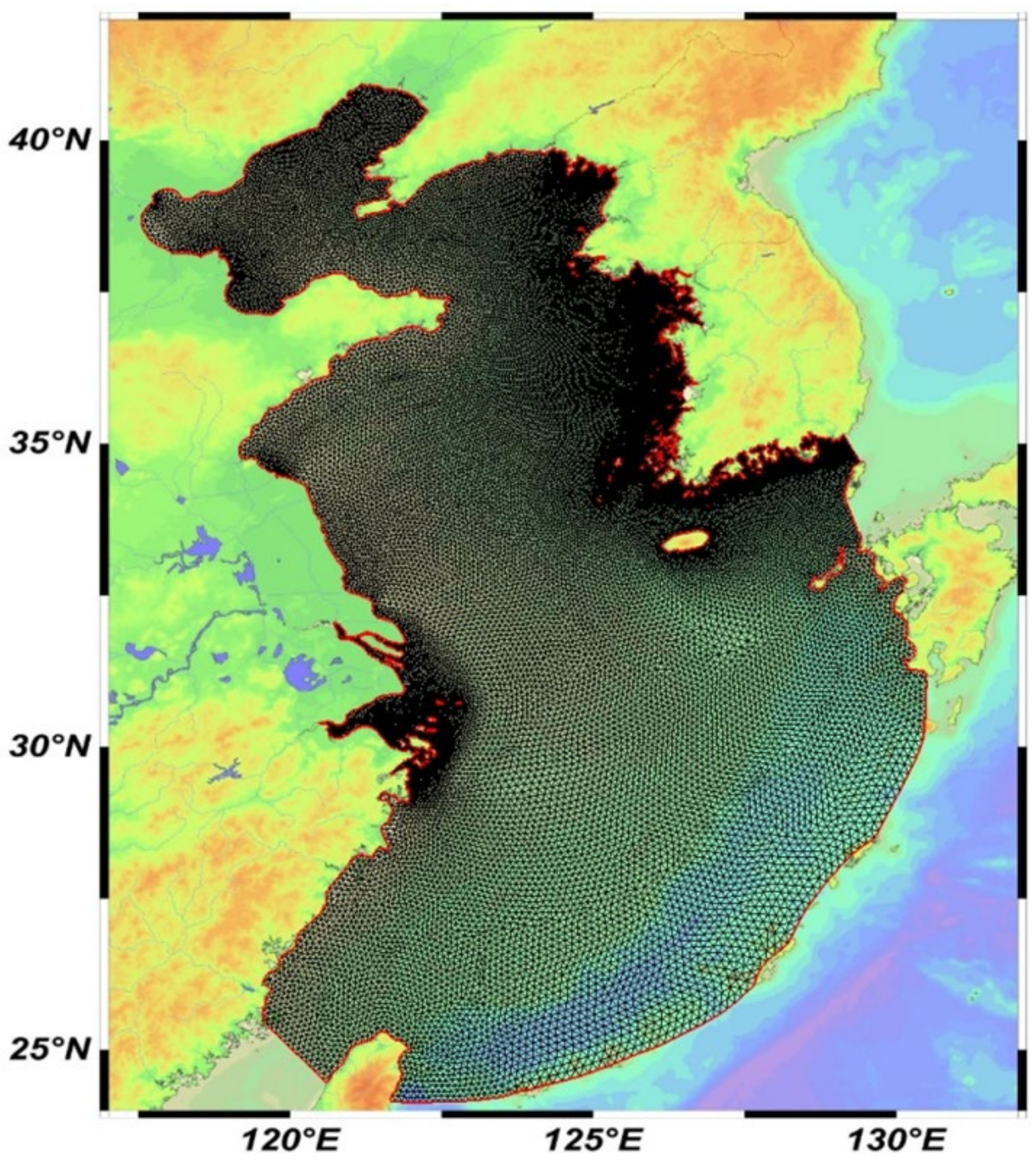

Fig.1 FEM meshes for YSECS

Major Hydrodynamic Inputs

For the open boundary conditions we have used results of global HYCOM simulations for the 2007-2011 years. Value α we have used has a range of values between 0.01 and 0.1. For η_t we have used NAO99 and TPXO-08. TPXO-08 global model database (http://volkov.oce.orst.edu/tides/global.html) contains 13 harmonics for the tidal elevations with resolution 1/30 degree. To calculate wind surface stresses and heat fluxes through the free surface the Era-Interim reanalysis data was used with 1.5° resolution.

Sedimentary Inputs

Suspended sediment (and freshwater) discharges from 6 main Yellow Sea rivers were used: Fuchun Jiang, Chan Jiang, Huai, Huang, Haiho and Han rivers. There are two main riverine outflows of suspended sediments, that is, ChianJiang and Huanghe. For ChianJiang 0.1 kg/m³ of clay, 0.2 kg/m³ of fine silt, 0.1 kg/m³ of coarse silt, 0.1 kg/m³ of fine sand, while for Huanghe 3.75 kg/m³ of clay, 10 kg/m³ of fine silt, 7.5 kg/m³ of coarse silt, 3.75 kg/m³ of fine sand.

For the bottom sediment input we assume that the distribution of sediment class parameter $\varphi(= -\log_2 d)$ takes a normal form (lognormal form for bed sediment size d), namely,

$$p(\varphi) = \frac{1}{\sqrt{2\pi}\,\sigma}\exp\left[-\frac{(\varphi-\varphi_{50})^2}{2\sigma^2}\right], \quad d_{50} = 2^{\varphi_{50}}$$

we then get the fraction of specific sediment ($\varphi_i < \varphi_{sp} < \varphi_{i+1}$) at each point

$$f(\varphi_{sp}) = \int_{\varphi_i}^{\varphi_{i+1}} \frac{1}{\sqrt{2\pi}\,\sigma}\exp\left[-\frac{(\varphi-\varphi_{50})^2}{2\sigma^2}\right] d\varphi$$

Using the φ_{50} distribution supplied by FIO(First Institute of Oceanography) and the sand fraction information prepared by Choi et al (2005b), we can determine the standard deviation numerically at each point (see Fig.2). Subsequently we have deduced horizontal maps of fractions of 5 sediment size classes (Fig. 3).

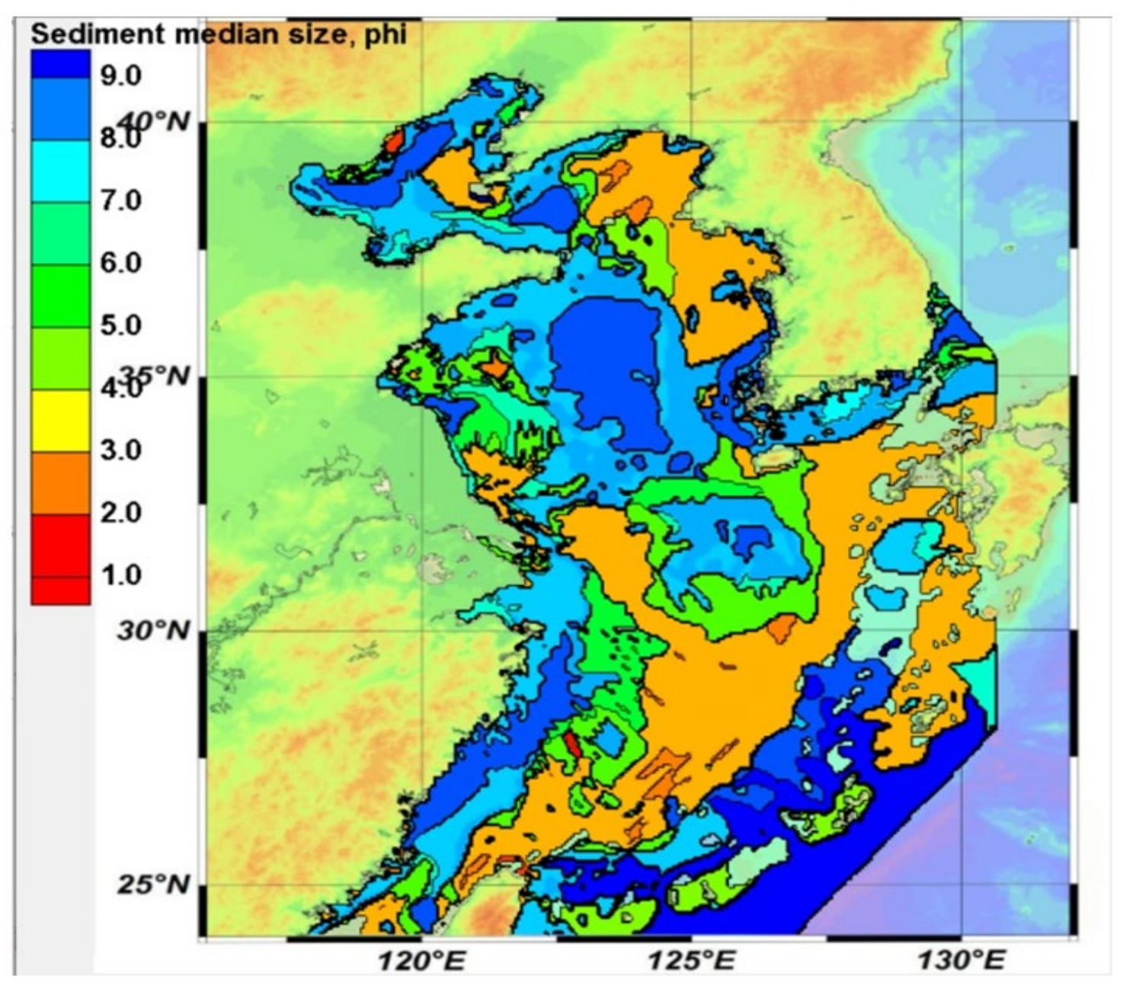

[φ_{50}]

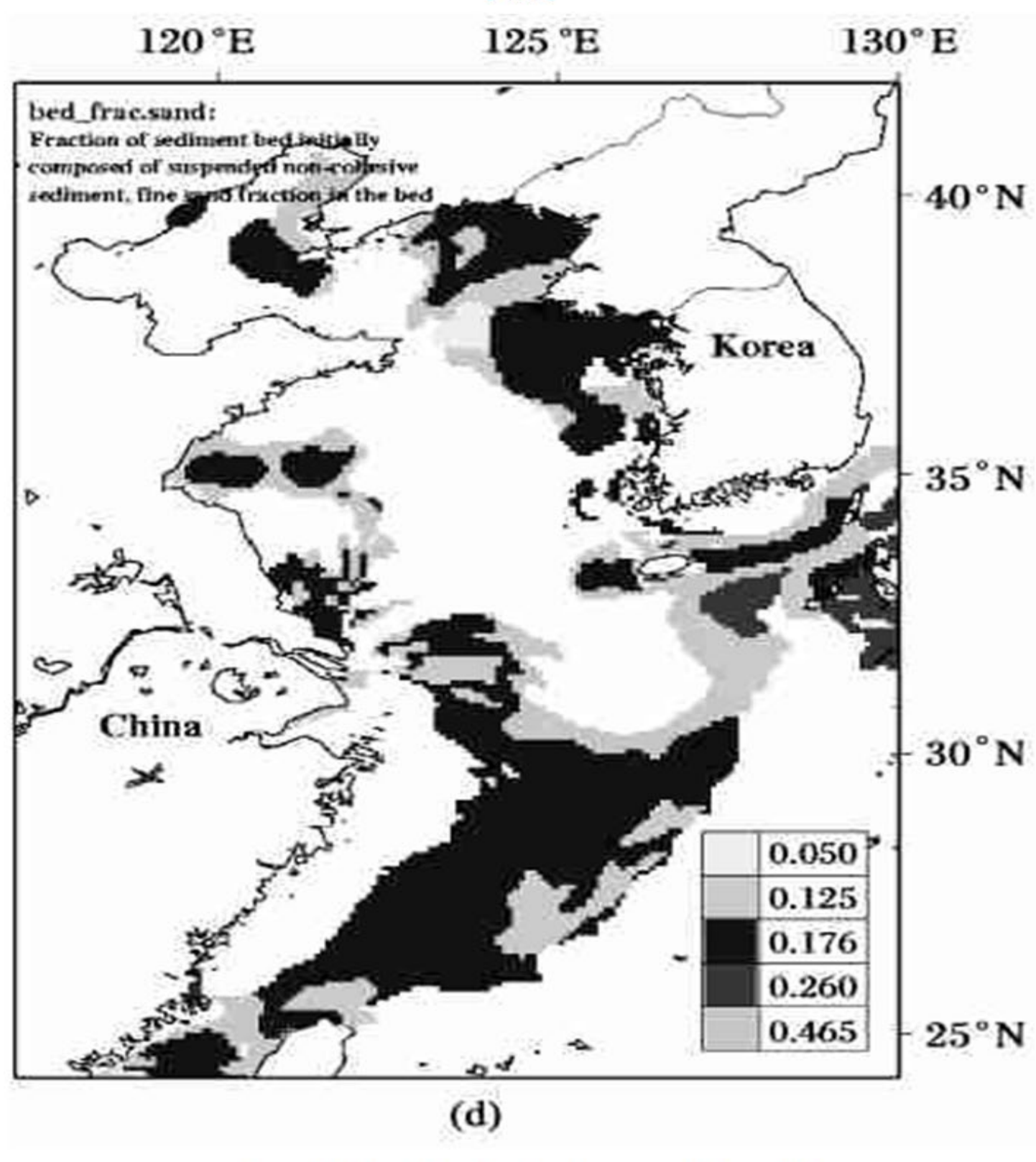

[sand fraction in bottom sediment]

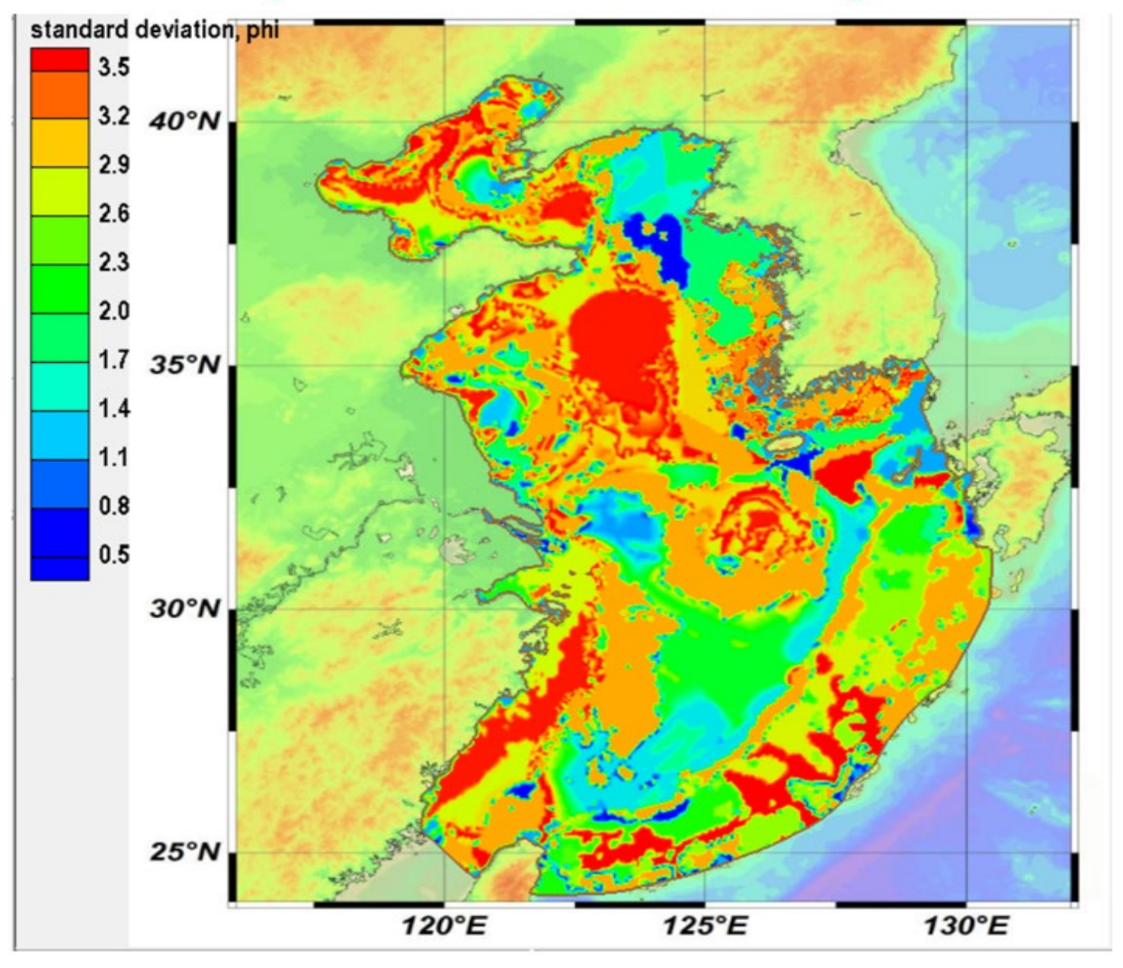

[computed standard deviation σ]

Fig.2 Distribution maps related to bottom sediment

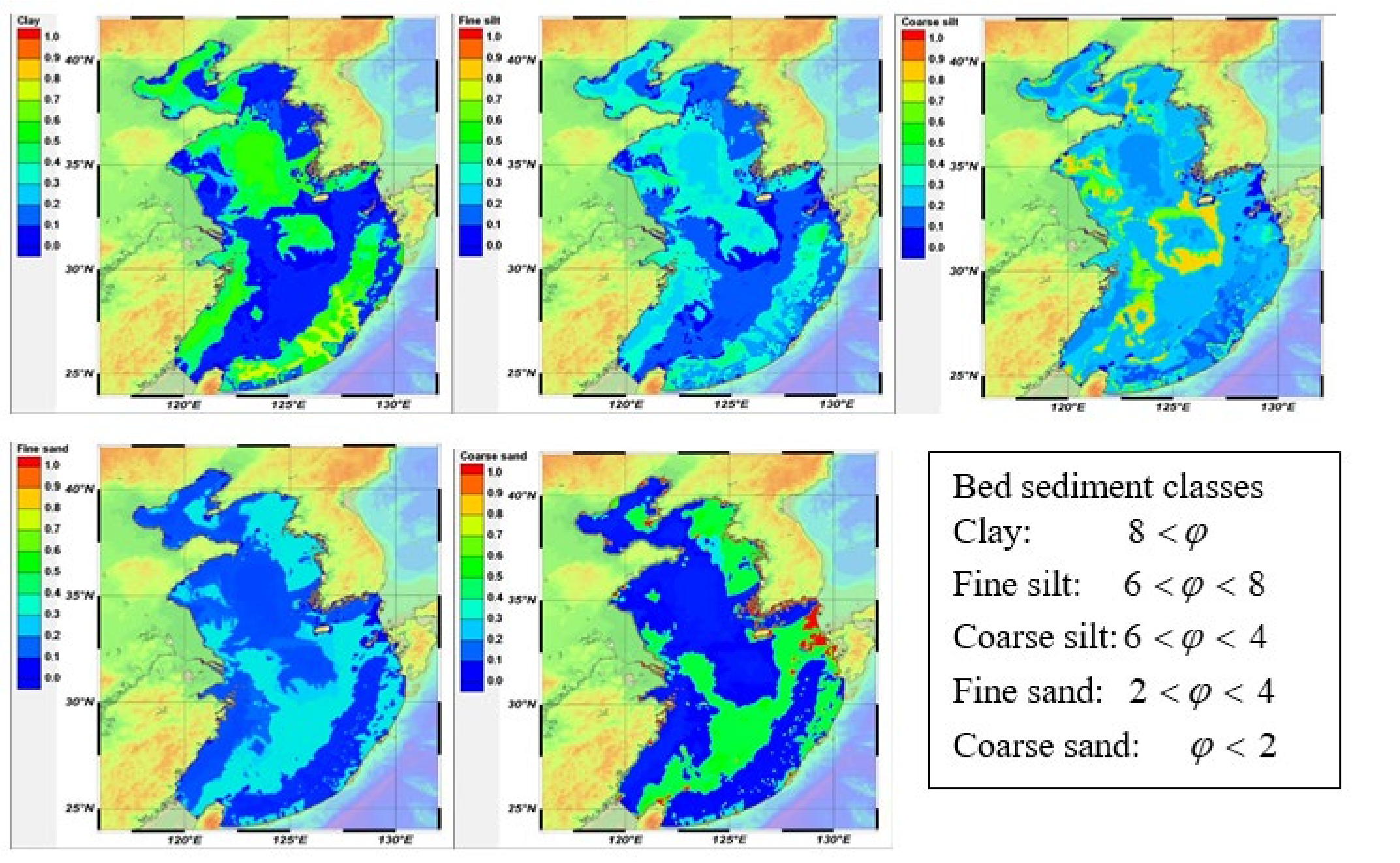

Bed sediment classes
Clay: $8 < \varphi$
Fine silt: $6 < \varphi < 8$
Coarse silt: $6 < \varphi < 4$
Fine sand: $2 < \varphi < 4$
Coarse sand: $\varphi < 2$

Fig.3 Distribution maps of fractions of five bed sediment classes

Simulated Results

Model results are in good agreement with tidal observations, known current schematic patterns, satellite images and previous model results (not shown here).

Fig.4 shows calculated wave fields during the passing of Muifa typhoon in August 2011. Computed significant wave heights was compared with buoy observations off the southwestern tip of Korean Peninsula (results not shown here).

Fig.5 show horizontal maps of suspended sediment concentrations at the sea surface obtained from GOCI images and model applications without wave and with waves for three different seasons. Concentrations from GOCI are in reasonable agreement with model results. Wave effects can be easily seen in Yangtze Bank region where high turbidity always occurs. As expected, inclusion of waves results in the increase of suspended sediment concentration in shallow coastal sea region and gradual decrease to the direction of offshore deep sea regions.

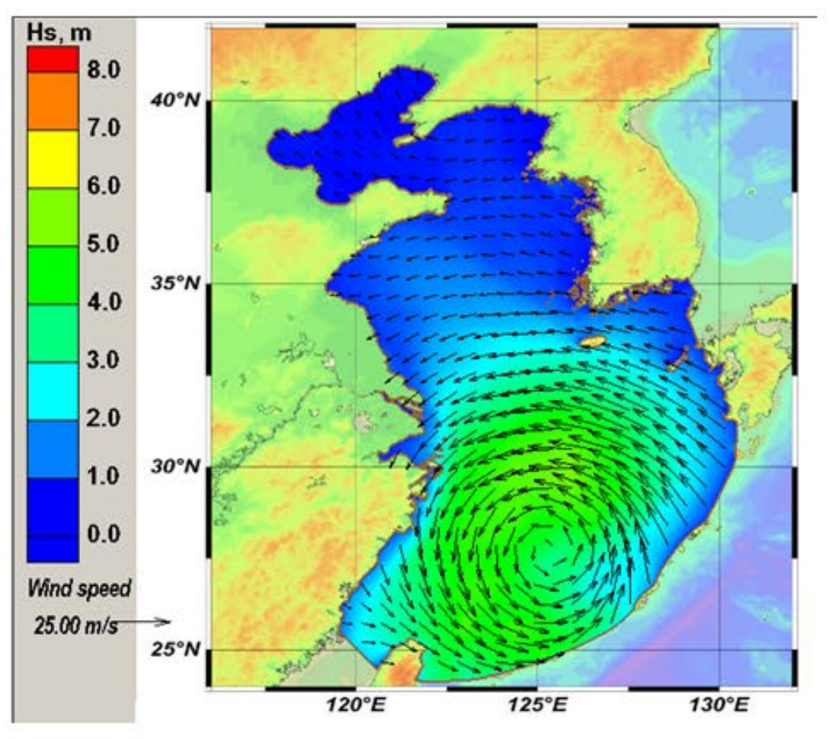

[Aug 6]

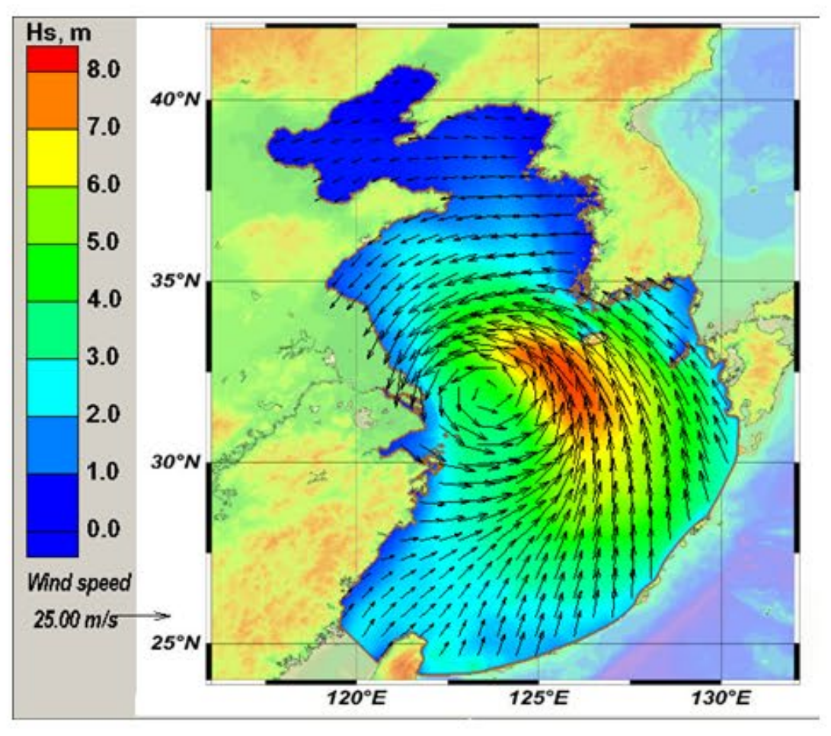

[Aug 7]

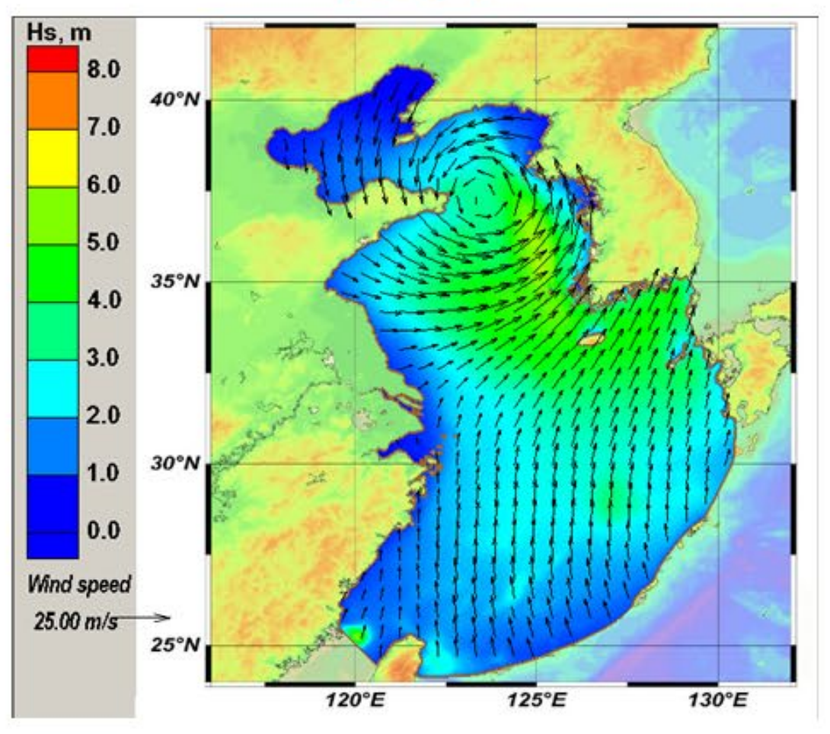

[Aug 8]

Fig.4 Computed distributions of significant wave heights during the passing of typhoon Muifa in 2011.

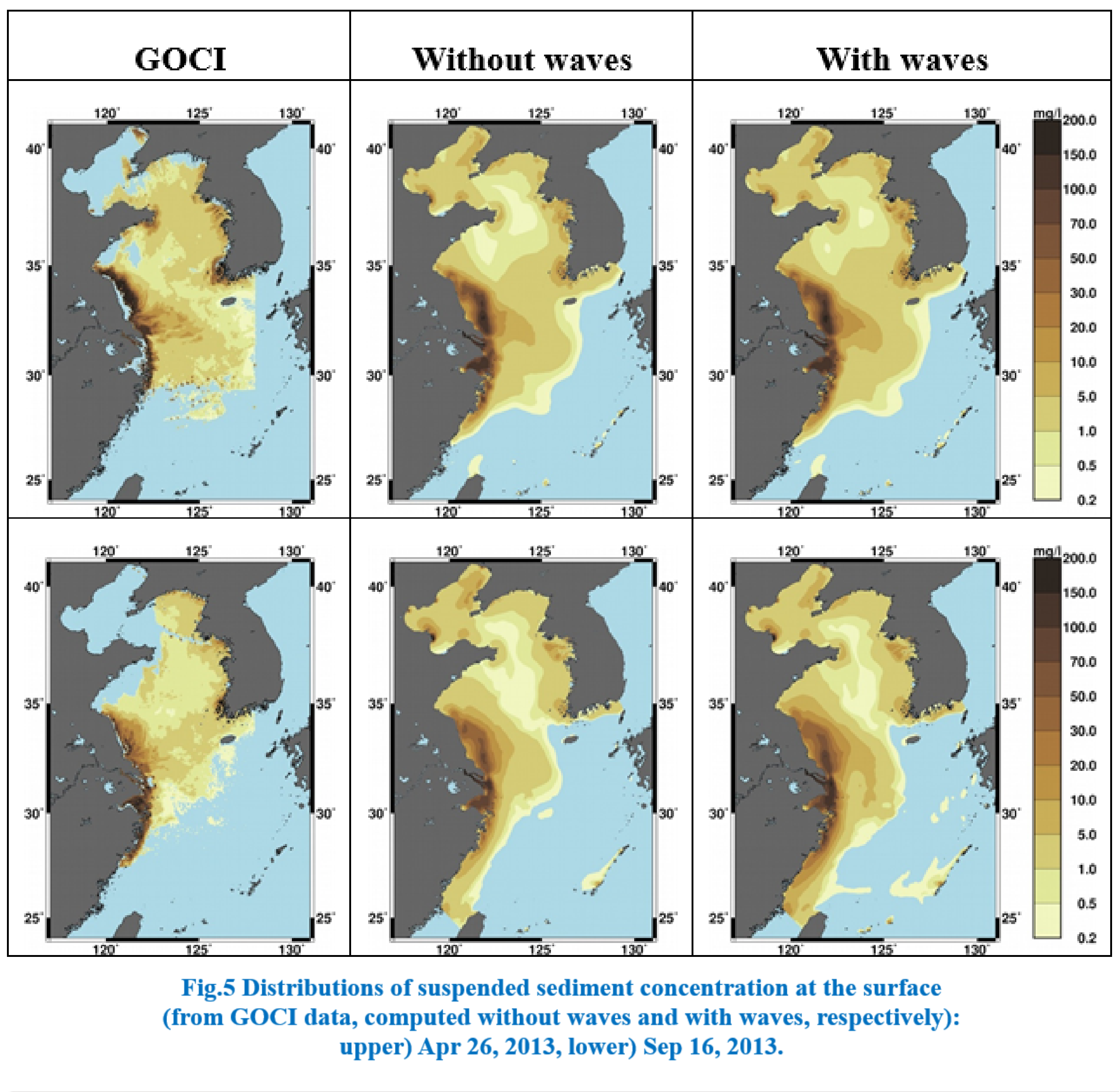

Fig.5 Distributions of suspended sediment concentration at the surface (from GOCI data, computed without waves and with waves, respectively): upper) Apr 26, 2013, lower) Sep 16, 2013.

CONCLUDING REMARKS

A 3D multi-scale circulation-wave-suspended sediment transport coupled modeling system applicable to the mixture of cohesive and non-cohesive sediments has been developed. Application to the YSECS has produced encouraging results. However, Further refinement of the model is obviously required through the shipboard measurements and remote sensing data related to suspended sediment.

References

Ariathurai, C.R., Arulanandan, K. 1978. J Hydraulics Division 104 (2): 279-282
Choi, B.-H., Moon, Yoon, J.-Y., Ko, J.-S., 2005a. Acta Oceanol. Sinica, 24, 1, 46-59.
Choi, B.-H., Moon, Yoon, J.-Y., Ko, J.-S., Yuk, J.-H., 2005b. China Ocean Eng., 19, 3, 235-250.
Roland, A., Zhang, Y.J., Wang, H.V. et al (2012). J. Geophys. Res., 117, C00J33
van Ledden, M., 2002. In: Winterwerp, H., Kranenburg, C. (Eds.), Fine Sediment in the Marine Environ., Elsevier, pp. 577–594.
van Rijn L.C. (1984). J. Hydr. Eng., 110, pp. 1613- 1641.